Monolithic phosphor-free InGaN/GaN quantum dot wavelength converter white light emitting diodes

Shafat Jahangir, Ines Pietzonka, Martin Strassburg, and Pallab Bhattacharya

Citation: Applied Physics Letters **105**, 111117 (2014); doi: 10.1063/1.4896304
View online: http://dx.doi.org/10.1063/1.4896304
View Table of Contents: http://scitation.aip.org/content/aip/journal/apl/105/11?ver=pdfcov
Published by the AIP Publishing

Monolithic phosphor-free InGaN/GaN quantum dot wavelength converter white light emitting diodes

Shafat Jahangir,[1] Ines Pietzonka,[2] Martin Strassburg,[2] and Pallab Bhattacharya[1,a)]
[1]*Center for Photonics and Multiscale Nanomaterials, Department of Electrical Engineering and Computer Science, University of Michigan, Ann Arbor, Michigan 48109-2122, USA*
[2]*OSRAM Opto Semiconductors GmbH, Leibnizstrasse 4, Regensburg, Germany*

(Received 22 July 2014; accepted 5 September 2014; published online 19 September 2014)

We report the characteristics of phosphor-free self-organized InGaN/GaN quantum dot wavelength converter white light emitting diodes grown by plasma assisted molecular beam epitaxy. The exciting quantum dots, in which electrically injected carriers recombine, are blue-emitting and the converter dots are red-emitting. We have studied the effect of tuning the number of dot layers and the peak emission wavelength of the exciting and converter dots on the nature of the emitted white light, in terms of the chromaticity coordinates and correlated color temperature. Depending on the values of these wavelengths, color temperatures in the range of 4420–6700 K have been derived at a current density of 45 A/cm^2 across multiple devices. The variation of the color temperature with change in injection current is found to be very small. © *2014 AIP Publishing LLC*.
[http://dx.doi.org/10.1063/1.4896304]

White light emitting diodes (LEDs) are systematically replacing incandescent bulbs and fluorescent lighting for a host of outdoor and indoor lighting applications due to the obvious advantages of low power consumption and long lifetime.[1,2] Monolithic planar white LEDs consisting of InGaN/GaN quantum wells, based on both direct electrical injection[3–7] as well as optical pumping in a converter scheme,[8] have been reported. Since long wavelength LEDs ($\lambda > 600$ nm) with III-nitride quantum well active regions are still in a developmental stage, the most common approach for realizing a solid state white LED is to either have a blue-emitting LED optically pump yellow phosphor[9,10] or have an ultraviolet (UV) LED excite rare earth doped blue-, green-, and red-emitting phosphors.[10] However, phosphor-converted white LEDs have distinct disadvantages. The conversion is inevitably accompanied by losses due to Stokes shift and non-radiative internal losses.[11] Backscattering of both pump and converted light by the phosphor gives rise to optical loss. Heating-related effects and the long-term reliability of the phosphors are additional detrimental factors.[12–15] A white LED with a monolithic semiconductor-based wavelength converter is therefore a desirable alternative. In contrast, InGaN/GaN self-organized quantum dots (QDs), grown in the Stranski-Krastanow mode by strain relaxation,[16] have significantly smaller piezoelectric polarization field and associated quantum confined Stark effect (QCSE) than those in comparable planar QWs.[17,18] Consequently, radiative carrier lifetimes in the dots are 10–100 times smaller than those in the wells.[17,19,20] Moreover, the quasi-three dimensional confinement of carriers in the InGaN/GaN QDs can reduce the rate of non-radiative recombination of carriers at dislocations and related defects. We have demonstrated red-emitting ($\lambda = 630$ nm) $In_{0.4}Ga_{0.6}N$/GaN self-organized quantum dot lasers, including a detailed characterization of their dc and small- and large-signal modulation properties.[20–22] We have also reported the characteristics of green-emitting ($\lambda = 524$ nm) QD light emitting diodes[17] and lasers.[23]

Here, we report the epitaxial growth, fabrication, and characteristics of phosphor-free InGaN/GaN quantum dot wavelength converter white LEDs. In the III-nitride device heterostructure, long wavelength $In_xGa_{1-x}N$/GaN ($0.35 \le x \le 0.38$) QD (580 nm $\le \lambda \le$ 615 nm) converters are optically pumped by blue light (432 nm $\le \lambda \le$ 450 nm) resulting from electrical injection of carriers and their recombination in $In_xGa_{1-x}N$/GaN ($0.22 \le x \le 0.24$) QDs to obtain white light emission. The electroluminescent properties of multiple devices have been measured. Chromaticity coordinates and correlated color temperatures (CCT) have been derived by analyzing the electroluminescence (EL) of the white LEDs at different injection current densities. The correlated color temperatures vary in the range of 4420–6700 K at a current density of 45 A/cm^2, depending on the wavelength of the blue and red emission from the respective quantum dots and the number of dot layers.

Phosphor-free InGaN/GaN QD wavelength converter white LED heterostructures, as shown schematically in Fig. 1(a), were grown on c-plane GaN-on-sapphire templates in a Veeco Gen 930 plasma assisted molecular beam epitaxy (PA-MBE) system equipped with standard Ga, In, Al, Mg, and Si effusion cells and a UNI-bulb nitrogen plasma source. The growth temperatures were monitored by an infrared pyrometer, calibrated by the (1×1) to (7×7) reflection high energy electron diffraction (RHEED) pattern transition at 880 °C on (111)-silicon. An n-doped (5×10^{18}cm^{-3}) 300 nm GaN buffer layer was first grown at a substrate temperature of 720 °C on c-plane n-GaN-on-sapphire templates for all samples. Multiple layers of self-organized InGaN/GaN QDs with 12 nm GaN barrier layers were grown as the long-wavelength converter over the n-GaN buffer layer under nitrogen rich condition at 541–550 °C. This was followed by the growth of 150 nm n-GaN layer ($n \sim 7.5 \times 10^{18}$cm^{-3}) at

a)E-mail: pkb@eecs.umich.edu

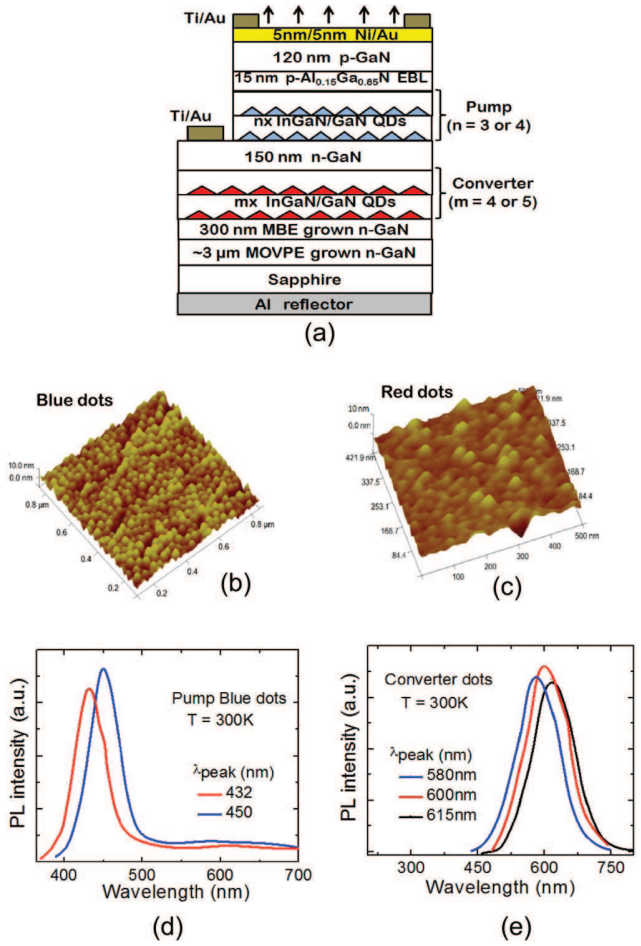

FIG. 1. (a) Schematic of InGaN/GaN quantum dot wavelength converter white LED heterostructure; atomic force microscopy images of self-organized $In_{0.24}Ga_{0.76}N$/GaN dots with peak emission at $\lambda = 450$ nm (b) and $In_{0.37}Ga_{0.63}N$/GaN dots with peak emission at $\lambda = 600$ nm (c); room temperature photoluminescence of blue-emitting pump dots (d); and red-emitting converter dots (e) incorporated in the LED heterostructure.

720 °C, multiple InGaN/GaN QD layers with 16 nm GaN barrier layers for blue emission grown at T = 585–592 °C, 15 nm p-$Al_{0.15}Ga_{0.85}N$ electron blocking layer (EBL), and finally a 120 nm p-GaN ($p \sim 7 \times 10^{17} cm^{-3}$) layer grown at 680 °C. The number of exciting and converter dot layers was carefully optimized to obtain true white emission. Also, the InGaN thickness to form the dots, the GaN barrier thickness and an interruption period under nitrogen flux were all optimized to maximize the dot radiative efficiency. Five device heterostructures were grown to investigate the tunability of white light emission from the LEDs by varying the number of exciting and converter $In_xGa_{1-x}N$ quantum dots and their alloy composition. Devices A–D have three excitation dot layers and five converter dot layers. In devices A, B, and C, the exciting quantum dot In content x was kept fixed at 0.24 for blue emission at $\lambda = 450$ nm and the converter dot emission wavelengths are 580, 600, and 615 nm, respectively (x = 0.35, 0.37, and 0.38). In device D, the exciting and converter dot emissions are at 432 nm (x = 0.22) and 580 nm, respectively. Device E contains four excitation dot layers ($\lambda = 432$ nm) and four converter dot layers ($\lambda = 580$ nm). Atomic force microscope (AFM) imaging was done on control QD samples grown under identical conditions to determine the structural characteristics of the dots. Figures 1(b) and 1(c) show AFM images of blue ($\lambda = 450$ nm) and red ($\lambda = 600$ nm) emitting QD layers. The blue dots have average height, base width, and areal density of 3 nm, 30 nm, and $\sim 4 \times 10^{10}$ cm^{-2}, respectively, while these parameters for the red converter dots are 4 nm, 40 nm, and $\sim 3.5 \times 10^{10}$ cm^{-2}, respectively. Figures 1(d) and 1(e) show measured room temperature photoluminescence (PL) spectra from blue- and red-emitting QD layers, respectively. The radiative efficiency η_r of the QDs was estimated from room- and low-temperature (10 K) PL intensities under saturation excitation, assuming that all non-radiative recombination channels are frozen at the lower temperature. The growth parameters of the blue- and red-emitting dots and their radiative efficiencies are listed in Table I. The emission wavelengths of exciting and converter dots in devices A–E and the device characteristics, to be described in the following, are listed in Table II.

Mesa-shaped LEDs of dimension 600 μm × 600 μm were fabricated using standard photolithography, reactive ion etching (RIE), and metallization techniques. Ti/Au (20 nm/200 nm) was deposited on top of the n-GaN region below the blue QD layers to form the n-contact and a thin semi-transparent Ni/Au (5 nm/5 nm) layer was evaporated and annealed (at 450 °C in 4:1 N_2:O_2) to form the p-contact on top of the p-GaN layer. Carriers are injected electrically into the blue-emitting InGaN/GaN QD layers and the emission from these dot layers optically excites the red-emitting converter dots to produce white light. An Al reflector layer is deposited on the backside sapphire surface. Figure 2(a) shows room temperature current-voltage characteristics of the LEDs. Turn-on voltages of ~5.5–6 V and series resistances of ~20–24 Ω are measured. White light emission of the phosphor-free LEDs can be tuned by using different combinations of pump and converter dot layers in the LED heterostructure. Figure 2(b) shows the optical micrograph of device B at an injection current density of 45 A/cm^2. Figure 2(c) illustrates device E emitting bluish white light at the same injection level. Figure 2(d) illustrates electroluminescence from device C as a function of injection current density. The two peaks at $\lambda = 450$ nm and 615 nm correspond to the exciting and converter QDs, respectively. Small blue-shifts in peak emission of ~4 nm and 7 nm, due to screening of the polarization field by injected carriers, are observed for the peaks at $\lambda = 450$ nm and 615 nm, respectively. The corresponding calculated polarization fields are 82 kV/cm and 170 kV/cm, respectively, which are significantly smaller than those reported for comparable planar InGaN quantum wells.[24,25] The smaller polarization field is a consequence of QD formation by strain relaxation. The measured light-current characteristics and the corresponding external quantum efficiency (EQE) of device C are depicted in Fig. 2(e). The efficiency reaches its peak value at an injection current density of 37 A/cm^2 in this device and at 45, 40, 42, and 44 A/cm^2 in devices A, B, D, and E, respectively. A reduction of 14%–17% in efficiency at an injection level of 100 A/cm^2 is observed in all the devices.

Electroluminescence intensities of the LEDs have been recorded with an Ocean Optics USB2000+ optical spectrum analyzer (with an optical resolution of 0.5 nm) to derive the

TABLE I. Growth parameters and radiative efficiencies of blue- and red-emitting InGaN/GaN self-organized quantum dots.

	Peak emission (nm)	Substrate T (°C)	In flux (Torr)	Ga flux (Torr)	In/III flux ratio	QD composition (%)	Radiative efficiency (%)
Exciting dots	432	592	3.4×10^{-8}	8.1×10^{-8}	0.3	22	54
	450	585	3.7×10^{-8}	7.8×10^{-8}	0.32	24	52
Converter dots	580	550	1.1×10^{-7}	1.04×10^{-7}	0.51	35	40
	600	545	1.12×10^{-7}	1×10^{-7}	0.53	37	44
	615	541	1.18×10^{-7}	9.94×10^{-8}	0.54	38	42

Commission Internationale de I'Eclairage (CIE) chromaticity coordinates and CCT of white light emission. As shown in Fig. 3(a), with increase in injection from 25 A/cm^2 to 100 A/cm^2 the CCT of device C changes by 210 K, from 4375 K to 4585 K, indicating better temperature stability of white light emission with injection current than that reported for InGaN/GaN multi-quantum well wavelength converter white LEDs.[8] Small blueshifts in peak emission of exciting and converter dots with increasing injection current contribute to the small increase in color temperature. The dependence of the correlated color temperature on injection current for devices A–E is illustrated in Fig. 3(b).

In our study, we have used the number of dot layers and their peak emission wavelength, for both exciting and converter QDs, as tuning parameters for the chromaticity coordinates and CCT of the emitted white light. The chromaticity coordinates and CCT for devices A–E at an injection current density of 45 A/cm^2 are listed in Table II and illustrated in Fig. 3(c). We found that the optimum number of dot layers were three for the exciting (blue) dots and five for the converter (red) dots. These were held constant for the devices A–D. Devices A, B, and C have the same excitation dot peak emission wavelength of 450 nm, but the converter dot peak emission wavelength increases by 35 nm from device A to C. As a result, the CCT for white light emission decreases by 930 K, with a value of 4420 K for device C at a current density of 45 A/cm^2. Using a converter dot peak emission $\lambda > 615$ nm will result in further decrease in CCT. The design of device D is similar to that of device A, except that the peak emission wavelength of the exciting dots is decreased to 432 nm. As a result, the CCT increases from 5350 K in device A to 5790 K in device D. Device E, which contains four excitation dot layers ($\lambda = 432$ nm) and four converter dot layers ($\lambda = 580$ nm), exhibits a bluish white emission with a CCT of 6700 K at a current density of 45 A/cm^2. The desirable values of CCT for high efficiency cool white and warm (soft) white light are ~4500 K and ~3000 K, respectively. These values of CCT would be difficult to achieve with all quantum well converter LEDs, since long wavelength ($\lambda > 600$ nm) emission with high radiative efficiency is difficult to achieve with such InGaN/GaN quantum wells due to increasing material inhomogeneities[26] and a strong polarization field.[27] A CCT ~ 5683 K has been reported for a white light converter LED in which blue-emitting QWs pump green-yellow emitting converter wells.[8] Correlated color temperatures of ~5900 K and ~5500 K have been reported for QW UV LED + blue-green-red phosphors and QW blue LED + yellow phosphor converter LEDs, respectively.[10] It is therefore evident that InGaN/GaN quantum dot converter LEDs may prove to be crucial for the realization of cool white and warm white light sources for a variety of applications.

TABLE II. CIE chromaticity coordinates and correlated color temperatures of wavelength converter white LEDs at an injection current density of 45 A/cm^2.

LEDs[a]	Pump dot emission λ (nm)	Converter dot emission λ (nm)	Chromaticity coordinates X	Chromaticity coordinates Y	CCT (K)
A	450	580	0.34	0.38	5350
B	450	600	0.35	0.37	4830
C	450	615	0.37	0.35	4420
D	432	580	0.33	0.36	5790
E	432	580	0.32	0.32	6700

[a]Devices A–D have three exciting dot and five converter dot layers. Device E has four exciting dot and four converter dot layers.

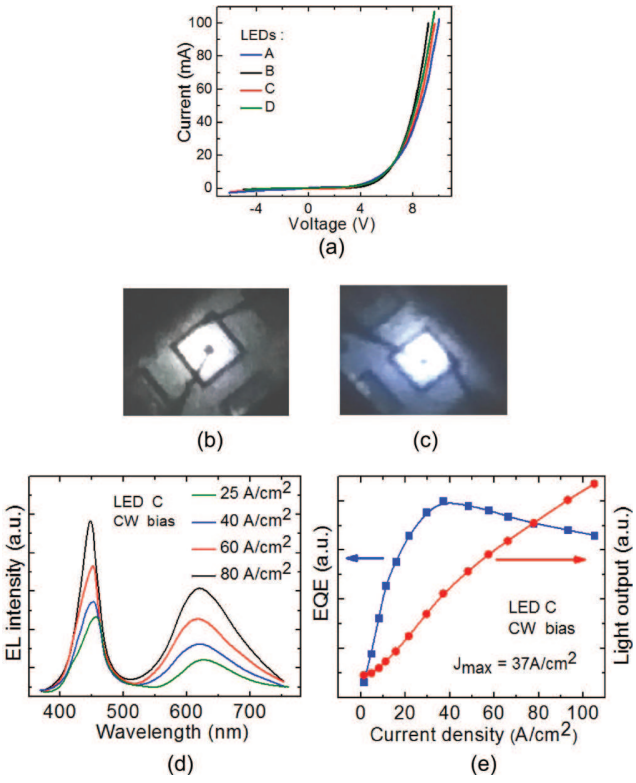

FIG. 2. (a) Measured current-voltage characteristics of white LEDs; optical micrographs of the devices biased at 45 A/cm^2: device C (b) and device E (c); (d) electroluminescence of device C as a function of injection current density; (e) light-current characteristics and external quantum efficiency of device C under CW biasing.

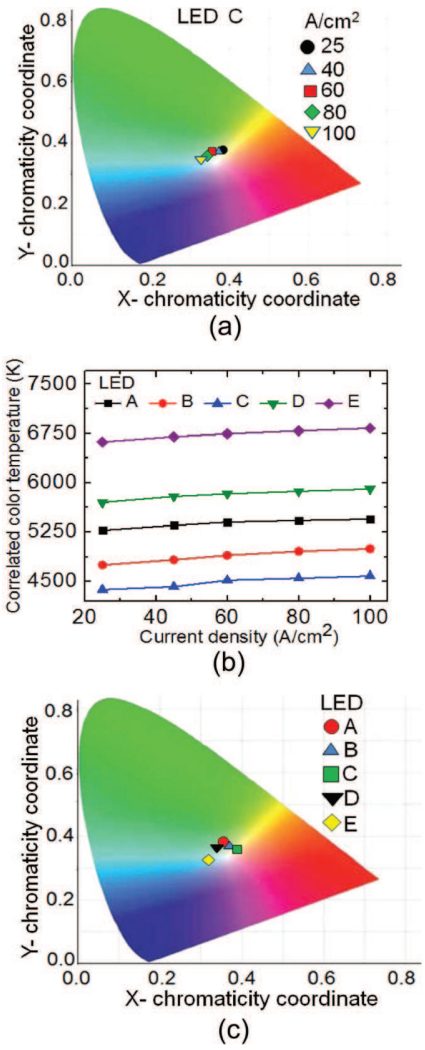

FIG. 3. (a) Trend of chromaticity coordinates of white light emission from device C with variation of injection current density; (b) variation of correlated color temperature of white light emission with injection current density for different LEDs. Solid lines are guides to the eye; (c) chromaticity coordinates of emission for different wavelength converter quantum dot white LEDs at a constant current density of 45 A/cm^2.

In conclusion, we demonstrate InGaN/GaN quantum dot wavelength converter white LEDs grown by plasma-assisted molecular beam epitaxy. Active blue-emitting quantum dot layers excite red-emitting converter quantum dot layers in these devices. We have studied the effect of varying the number of dot layers and the peak emission wavelength of the excitation and converter dots. As a result, the correlated color temperature of the white LEDs varies from 4420 K to 6700 K at an injection current density of 45 A/cm^2, with the lower value resulting from a device with excitation and converter dots having peak emissions at 450 nm and 615 nm, respectively.

The work was supported in part by the National Science Foundation Materials Research Science and Engineering Center (MRSEC) program under Grant DMR-1120923 and in part by the European Community within the FP7 Project "NEWLED" (Contract No. 318388).

[1]E. F. Schubert and J. K. Kim, Science **308**, 1274 (2005).
[2]R. Hu, X. B. Luo, H. Feng, and S. Liu, J. Lumin. **132**, 1252 (2012).
[3]B. Damilano, N. Grandjean, C. Pernot, and J. Massies, Jpn. J. Appl. Phys., Part 1 **40**, 918 (2001).
[4]M. Yamada, Y. Narukawa, and T. Mukai, Jpn. J. Appl. Phys., Part 1 **41**, 246 (2002).
[5]C. F. Huang, C. F. Lu, T. Y. Tang, J. J. Huang, and C. C. Yang, Appl. Phys. Lett. **90**, 151122 (2007).
[6]I. K. Park, J. Y. Kim, M. K. Kwon, C. Y. Cho, J. H. Lim, and S. J. Park, Appl. Phys. Lett. **92**, 091110 (2008).
[7]S. N. Lee, H. S. Paek, H. Kim, T. Jang, and Y. Park, Appl. Phys. Lett. **92**, 081107 (2008).
[8]B. Damilano, P. Demolon, J. Brault, T. Huault, F. Natali, and J. Massies, J. Appl. Phys. **108**, 073115 (2010).
[9]S. Nakamura and G. Fasol, *The Blue Laser Diode* (Springer-Verlag, Berlin, Germany, 1997), pp. 216–219.
[10]J. K. Sheu, S. J. Chang, C. H. Kuo, Y. K. Su, L. W. Wu, Y. C. Lin, W. C. Lai, J. M. Tsai, G. C. Chi, and R. K. Wu, Photonics Technol. Lett. **15**, 18 (2003).
[11]M. Huang and L. Yang, Photonics Technol. Lett. **25**, 1317 (2013).
[12]T. Tamura, T. Setomoto, and T. Taguchi, J. Lumin. **87–89**, 1180 (2000).
[13]J. H. Hwang, Y. D. Kim, J. W. Kim, S. J. Jung, H. K. Kwon, and T. H. Oh, Phys. Status Solidi C **7**, 2157 (2010).
[14]Q. Zhang, F. Jiao, Z. Chen, L. Xu, A. Wang, and S. Liu, J. Semicond. **32**, 012002 (2011).
[15]C. Yuan and X. B. Luo, Int. J. Heat Mass Transfer **56**, 206 (2013).
[16]B. Damilano, N. Grandjean, S. Dalmasso, and J. Massies, Appl. Phys. Lett. **75**, 3751 (1999).
[17]M. Zhang, P. Bhattacharya, and W. Guo, Appl. Phys. Lett. **97**, 011103 (2010).
[18]S. Schulz and E. O'Reilly, Phys. Rev. B **82**, 033411 (2010).
[19]Y. Wu, Y. Lin, H. Huang, and J. Singh, J. Appl. Phys. **105**, 013117 (2009).
[20]T. Frost, A. Banerjee, K. Sun, S. L. Chuang, and P. Bhattacharya, IEEE J. Quantum Electron. **49**, 923 (2013).
[21]T. Frost, A. Banerjee, and P. Bhattacharya, Appl. Phys. Lett. **103**, 211111 (2013).
[22]T. Frost, A. Banerjee, S. Jahangir, and P. Bhattacharya, Appl. Phys. Lett. **104**, 081121 (2014).
[23]M. Zhang, A. Banerjee, C. S. Lee, J. M. Hinckley, and P. Bhattacharya, Appl. Phys. Lett. **98**, 221104 (2011).
[24]Y. D. Jho, J. S. Yahng, E. Oh, and D. S. Kim, Phys. Rev. B **66**, 035334 (2002).
[25]D. Queren, A. Avramescu, G. Bruderl, A. Breidenassel, and M. Schillgalies, Appl. Phys. Lett. **94**, 081119 (2009).
[26]Y. H. Cho, G. H. Gainer, A. J. Fischer, J. J. Song, S. Keller, U. K. Mishra, and S. P. DenBaars, Appl. Phys. Lett. **73**, 1370 (1998).
[27]C. Y. Lai, T. M. Hsu, W. H. Chang, K. U. Tseng, C. M. Lee, C. C. Chuo, and J. I. Chyi, Phys. Status Solidi B **228**, 77 (2001).